Generalized $\vec{k}\cdot\vec{p}$ interpolation method for electronic wave functions: Positron annihilation spectra of ferromagnetic iron

H. J. F. Jansen*
Materials Science Center, Solid State Physics Laboratory, University of Groningen, Groningen, The Netherlands

F. M. Mueller
Research Institute for Materials, University of Nijmegen, Toernooiveld, Nijmegen, The Netherlands

(Received 23 November 1981)

We have extended our generalized $\vec{k}\cdot\vec{p}$ interpolation scheme to wave functions. The speed of this method with wave functions was about 200 times faster than the Korringa-Kohn-Rostoker method. All matrix elements of interest were accurate on a 5% or better scale. As an example we calculate the positron annihilation spectra of ferromagnetic iron. This is a typical case where the matrix elements of the annihilation process play a dominant role, since some of the bands near the Fermi level have pronounced *s-p* character.

I. INTRODUCTION

The interpolation of energy eigenvalues in electronic band theory is a well-studied problem. Less well characterized is the problem of interpolating wave functions and their matrix elements. However, this aspect is equally important since matrix elements are basic ingredients for the evaluation of almost all physically observable quantities. In this paper we consider an accurate and fast interpolation method for wave functions and we apply this method to calculate positron annihilation spectra of ferromagnetic iron.

In principle, wave functions can be derived from every interpolation method, such as pseudopotentials,[1] parametrized tight binding or Slater-Koster schemes,[2] or combined schemes.[3] The description of wave functions through $\vec{k}\cdot\vec{p}$ perturbation theory is particularly straightforward and simple.[4] We have expanded our study of the generalized $\vec{k}\cdot\vec{p}$ interpolation method[5] to approximate wave functions as well as eigenvalues. Not too surprising, it turns out that the accuracy of the interpolated wave functions is less: Nevertheless the method is sufficiently accurate to be useful, and is quite fast.

Experiments studying the annihilation of thermal positrons in solids provide us information concerning energy levels as well as wave functions.[6] This powerful technique is founded upon the imaging of the properties of the annihilated electron in the final gamma quanta. Experiments measuring the total momentum of the photons are very well described by electron band theory, since sampling the electrons in reciprocal space focusses on the itinerant character of the electrons. We have evaluated positron annihilation spectra of ferromagnetic iron, using a new, parametrized band structure of ferromagnetic iron which was constructed to accurately describe the results of de Haas–van Alphen technique measurements.[7,8] We compare our results with the available experimental data.[9]

The plan of this paper is as follows. Section II recapitulates the basic formulas of our generalized $\vec{k}\cdot\vec{p}$ interpolation method. Section III describes the interpolation of wave functions. In Sec. IV we discuss the accuracy of our interpolated matrix elements for positron annihilation by comparing them with matrix elements evaluated by a Korringa-Kohn-Rostoker (KKR) method. In Sec. V we show our results for positron annihilation spectra of ferromagnetic iron, while Sec. VI shows our conclusions.

II. GENERALIZED $\vec{k}\cdot\vec{p}$ INTERPOLATION

The relation between the band structure in two points in reciprocal space is furnished by $\vec{k}\cdot\vec{p}$ perturbation theory.[4] If the energy eigenvalues and wave functions are known for a specific value of the wave vector $\vec{K}$ one can deduce the band struc-

ture in a general point $\vec{k}$ by diagonalizing the $\vec{k}\cdot\vec{p}$ Hamiltonian

$$H_{ij}(\vec{k},\vec{K})=[E_i(\vec{K})+(\vec{k}-\vec{K})^2]\delta_{ij} +2(\vec{k}-\vec{K})\cdot\vec{p}_{ij}(\vec{K}) . \quad (1)$$

Here $(\vec{p}_{ij}(\vec{K})$ are the matrix elements of the momentum operator, and $E_i(\vec{K})$ is the energy eigenvalue for band i.

In many cases one is interested only in bands in the immediate vicinity of the Fermi level. This allows us to approximate the full $\vec{k}\cdot\vec{p}$ Hamiltonian by a matrix of finite rank; the size of this matrix determines the accuracy of the resulting eigenvalues. In the case of narrow bands the quality of the evaluated eigenvalues is poor and an extrapolation over a full zone of the band structure is inaccurate.[10]

Fortunately the number or bands to be described is often small. Then it is convenient to reduce the size of the model Hamiltonian matrix to the number of bands of interest. This can be done most simply by applying Löwdin perturbation theory.[11] We separate the energy bands into two classes, class A containing the bands of interest and class B containing all other bands. We define the Löwdin matrix U by

$$U_{nm}(E,\vec{k},\vec{K})=H_{nm}(\vec{k},\vec{K})+\sum_{\substack{l\in B\\ 1\neq n,m}}\frac{H_{nl}(\vec{k},\vec{K})H_{lm}(\vec{k},\vec{K})}{E-H_{ll}(\vec{k},\vec{K})}+\sum_{\substack{lj\in B\\ n\neq 1\\ l\neq j\\ j\neq m}}\frac{H_{nl}(\vec{k},\vec{K})H_{lm}(\vec{k},\vec{K})H_{jm}(\vec{k},\vec{K})}{[E-H_{ll}(\vec{k},\vec{K})][E-H_{jj}(\vec{k},\vec{K})]}+\cdots . \quad (2)$$

The eigenvalue problem then reduces to diagonalizing a matrix of the size of class A,

$$\sum_{m\in A}U_{nm}(E,\vec{k},\vec{K})c_m=Ec_n,\quad n\in A , \quad (3)$$

while the elements of the eigenvector in class B are determined by

$$c_n=\sum_{m\in A}\frac{U_{nm}(E,\vec{k},\vec{K})}{E-H_{nn}(\vec{k},\vec{K})}c_m,\quad n\in B . \quad (4)$$

The Löwdin matrix U is a function of the wave vector $\vec{k}$ and can be expanded in symmetry adapted polynomials which are centered at $\vec{K}$:

$$U_{nm}(E,\vec{k},\vec{K})=\sum_l C^l_{nm}(E,\vec{K})p_l(\vec{k}-\vec{K}) . \quad (5)$$

The crystal symmetry of the electronic band structure is reflected in the coefficients C. Using the Wigner-Eckart theorem these are factorized into the product of a generalized Clebsch-Gordon coefficient and a reduced matrix element. In our previous paper[5] we have shown that these reduced matrix elements can be used as free parameters for a fast and accurate interpolation of the energy eigenvalues of the electronic band structure.

III. INTERPOLATION OF WAVE FUNCTIONS

Of course the use of the $\vec{k}\cdot\vec{p}$ Hamiltonian is not restricted to the evaluation of energy bands alone. Wave functions may be obtained directly from the eigenvectors of the $\vec{k}\cdot\vec{p}$ Hamiltonian

$$\sum_j H_{ij}(\vec{k},\vec{K})d_j(n\vec{k},\vec{K})=E_n(\vec{k})d_i(n\vec{k},\vec{K}) , \quad (6)$$

$$\psi(n\vec{k},\vec{r})=e^{i(\vec{k}-\vec{K})\vec{r}}\sum_j d_j(n\vec{k},\vec{K})\psi(j\vec{K},\vec{r}) . \quad (7)$$

The accuracy of the interpolated wave functions can be simply estimated by the following argument. Suppose the interpolated wave function $\tilde{\psi}$ differs from the exact wave function ψ by an amount $\delta\psi$,

$$\tilde{\psi}=\psi+\delta\psi . \quad (8)$$

Because of orthogonality we have

$$\psi\delta\psi=0 . \quad (9)$$

The difference between the interpolated energy $\tilde{\epsilon}$ and the exact energy ϵ then becomes

$$\tilde{\epsilon}-\epsilon=\delta\psi H\delta\psi , \quad (10)$$

where (9) is used together with the fact that ψ obeys Schrödinger's equation. Hence as is well known the error in wave function is of first order, while the error in the energy is of second order. The typical accuracy of the energy in a global fit is in the range $0.1-1.0\,\%$ and consequently the error in the wave function is expected to be $2-3\,\%$.

Wave functions abound in information compared with the energy bands. It is neither feasible nor desirable to define the accuracy of a wave function. All one really wants to know is the accuracy of the

description of experimentally observable quantities, due to the errors in the matrix elements. Hence, model wave functions have to be tested for each new application again and again by comparing matrix elements obtained by integrating *ab initio* wave functions and model wave functions.

The derivation of the $\vec{k}\cdot\vec{p}$ Hamiltonian (1) uses the orthogonality of the basis functions

$$\int d^3r\, u^*(n\vec{K},\vec{r})u(m\vec{K},\vec{r})=\delta_{nm}\ . \tag{11}$$

This relation leaves the phase of the wave functions undetermined. However, the relative phases of the components of the eigenvectors of the model Hamiltonian are fixed and do not allow any variation in the relative phases of the basis function. The question arises which value of the angle $\zeta(j\vec{K})$ has to be used in the expansion

$$\psi(n\vec{k},\vec{r})=e^{i(\vec{k}-\vec{K})\cdot\vec{r}}\sum_j d_j(n\vec{k},\vec{K})e^{i\zeta(j\vec{K})} \times\psi(j\vec{K},\vec{r})\ . \tag{12}$$

Equivalently one can ask which values of the relative phases of the basis functions are consistent with the fitted values of the parameters in the model Hamiltonian.

Löwdin's formula shows that the phase factors of basis functions belonging to class B are not important since these basis functions only appear in combinations of the form $\psi^*\psi$. Phase factors of wave functions belonging to class A are determined by comparing eigenvectors of the model Hamiltonian with values derived from *ab initio* eigenfunctions near the points of high symmetry. We have

$$d_j(n\vec{k},\vec{K})=\int d^3r\, u^*(j\vec{K},\vec{r})u(n\vec{k},\vec{r})\ . \tag{13}$$

In case of potentials with inversion symmetry the coefficients d can be chosen real for real values of the parameters. Consistently, plane-wave expansions of the wave functions have real coefficients and phase differences become mere sign differences. The relative sign of basis functions at points of high symmetry can be unambiguously determined by comparing values obtained via (13) with model eigenvectors.

A second problem is the evaluation of the matrix elements of the model Hamiltonian U connecting the basis states of class A and class B. Since the influence of basis functions belonging to class B is relatively small (less than 20% for the cases we have investigated) it is sufficient to take the influence of class B into account only up to first or-

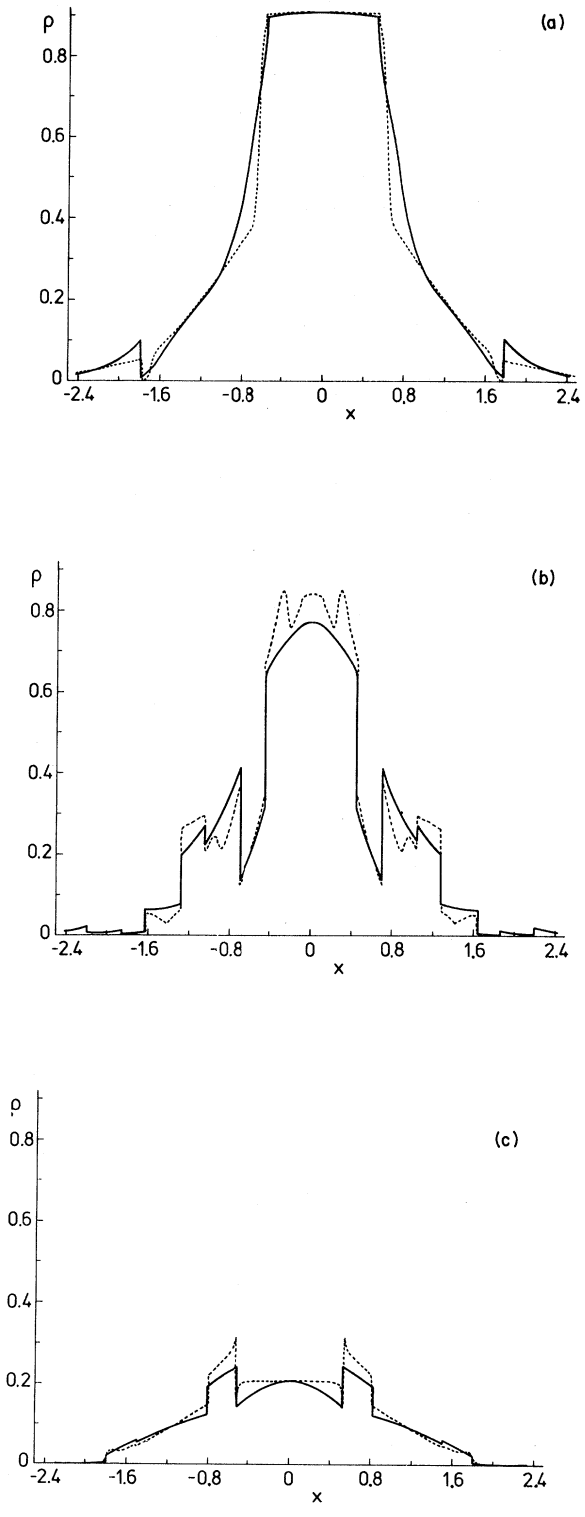

FIG. 1. (a) Positron annihilation momentum density with $\vec{q}=(0,0,x)$ a.u.; solid lines are obtained from *ab initio* results, dashed lines from interpolated wave functions. (b) See (a). $q=(0.581\,16,0,x)$ a.u. (c) See (a). $q=(1.162\,33,0,x)$ a.u.

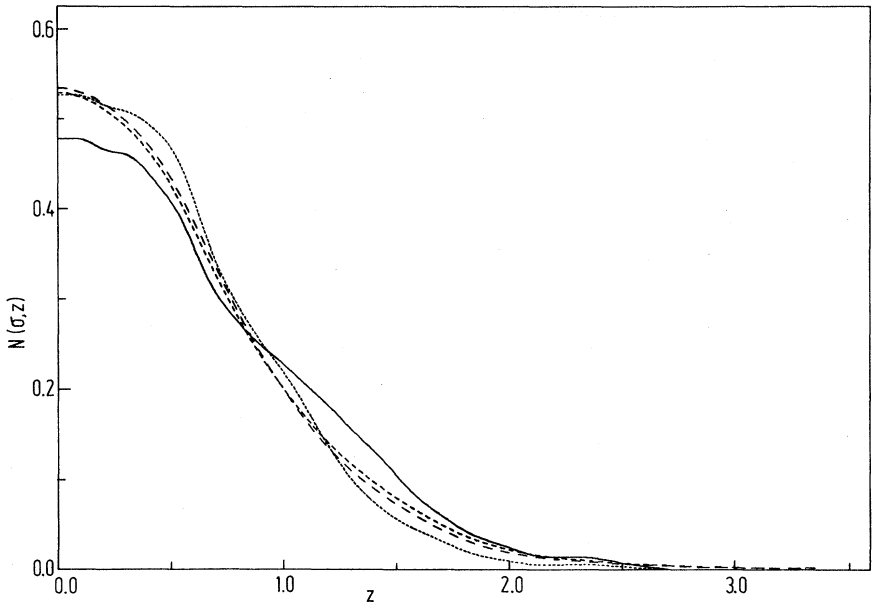

FIG. 2. Twice-integrated positron annihilation spectra along $\hat{s}$ near [100]. Theoretical results are given by the solid line (majority spin) and the short dashes (minority spin); experimental results are given by the medium-sized dashes (majority spin) and the long dashes (minority spin).

der of the expansion given in Eq. (2), and using previously defined quantities,

$$d_j(n\vec{k},\vec{K})=\sum_{j'\in A} d_{j'}(n\vec{k},\vec{K})\frac{2(\vec{k}-\vec{K})\cdot\vec{P}_{jj'}(\vec{K})}{E(n\vec{k})-E(j\vec{K})}\,, \qquad j\in B \quad (14)$$

using *ab initio* values for the matrix elements of the momentum operator. One has to determine by trial and error how many elements from class B must be used in expansion (14). In the cases we have investigated this number turned out to be of the same order as the number of elements in class A. Phase problems do not occur, since the matrix elements are constructed from *ab initio* wave functions.

Smooth interpolation throughout the first Brillouin zone is accomplished by applying the same type of Gaussian weight factors as was used previously for the energy values[5]:

$$\psi(n\vec{k},\vec{r})=\frac{\sum_{\vec{K}}\exp[-\alpha(\vec{k}-\vec{K})^2/r^2(\vec{K})]\psi_{\vec{K}}(n\vec{k},\vec{r})}{\sum_{\vec{K}}\exp[-\alpha(\vec{k}-\vec{K})^2/r^2(\vec{K})]}\,, \quad (15)$$

where the wave functions $\psi_{\vec{K}}(n\vec{k},\vec{r})$ refer to the point of high symmetry $\vec{K}$. The summations incorporate all points of high symmetry $\vec{K}$ used for model Hamiltonian expansions. $r(\vec{K})$ is the range of the expansion centered at $\vec{K}$. α can be chosen freely to give an optimal results. It is a necessary condition that the wave functions $\psi(j\vec{K},\vec{r})$ at different points of high symmetry are phased coherent. This can be easily achieved by following the phase of *ab initio* wave functions along lines connecting the points of high symmetry. The errors in the approximate wave function appear in their radial part, since their angular variation was constructed through symmetry projectors, and is exact.

The deviations in the radial parts of the wave function are primarily caused by their energy dependence: We have approximated this by the

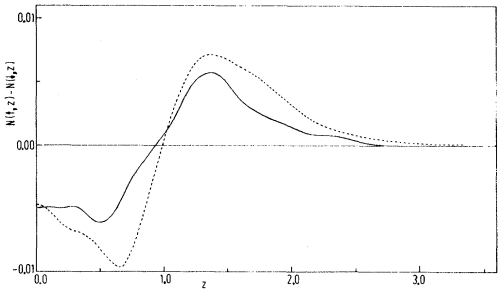

FIG. 3. Difference between the majority- and minority-spin spectra along $\hat{s}$ near [100]. The theoretical results (solid line) are multiplied by 0.1. Dashed line indicates the experimental results.

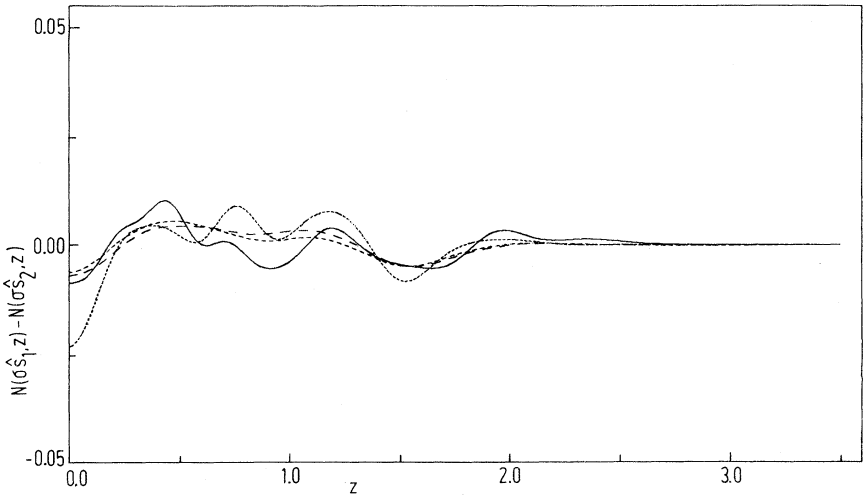

FIG. 4. Difference between the spectra along two directions, $\hat{s}_1$ near [211] and $\hat{s}_2$ near [421]. Theoretical results are given by the solid line (majority spin) and the short dashes (minority spin); experimental results are given by the medium-sized dashes (majority spin) and the long dashes (minority spin).

few values at $\vec{K}$. Such errors could be made smaller by including more states belonging to class B and by improving on the matrix elements of U connecting class A and B. The error in the radial part of the wave functions is largest for wave vectors along lines of high symmetry since in that case the mixing of the basis functions is restricted by symmetry so that states distant in energy play a role.

All matrix elements of our interest turned out to be accurate on a 5% or better scale. This is a consequence of the necessary quadratures in direct or in reciprocal space, which tend to average such errors. The speed of this method with wave functions was about 200 times faster than that of the original KKR scheme.[5,7]

IV. MATRIX ELEMENTS FOR POSITRON ANNIHILATION

We have applied our interpolation method to evaluate the photon momentum distribution as measured in a positron annihilation experiment.

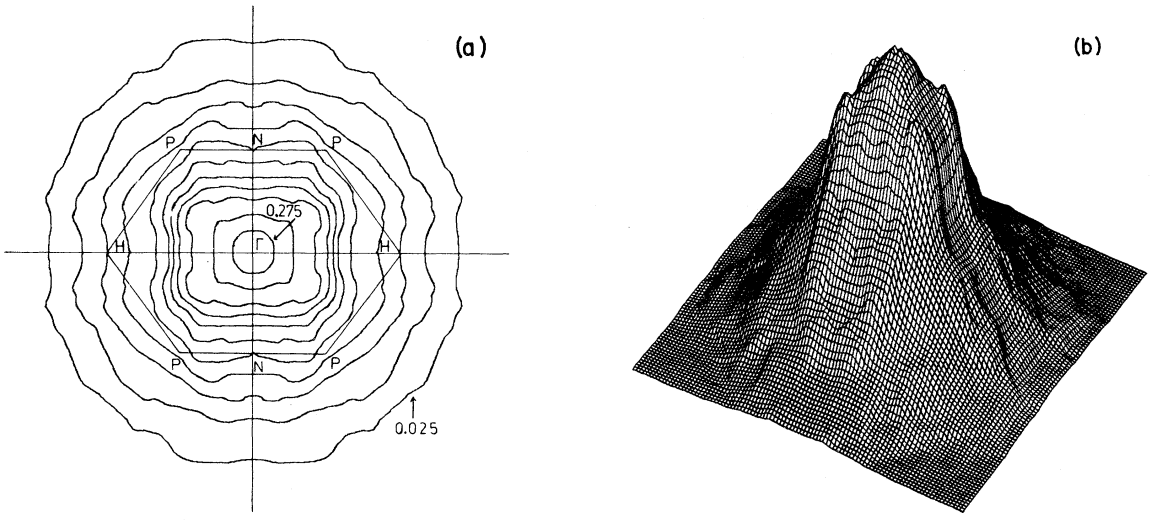

FIG. 5. (a) Contours of the total once-integrated positron annihilation spectrum, $[N(\uparrow,\hat{s}\,\vec{t})+N(\downarrow,\hat{s},\vec{t})]/2$ in a (110) plane. First Brillouin zone is also shown. Subsequent contours differ by 0.025. (b) Three-dimensional plot of (a).

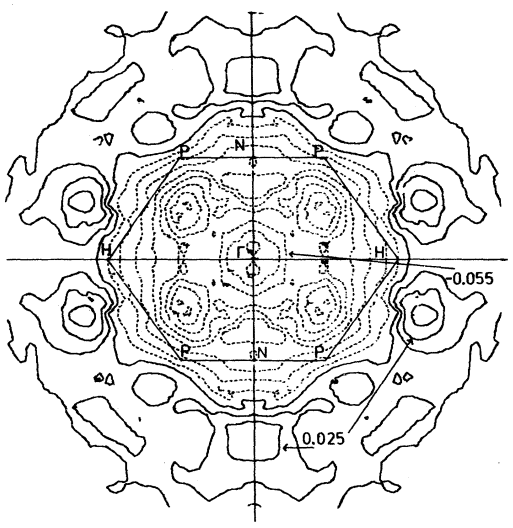

FIG. 6. Contours of the spin difference of the once-integrated positron annihilation spectra, $N(\uparrow,\hat{s},\hat{t})-N(\downarrow,\hat{s}\hat{t})$ in a (110) plane. First Brillouin zone is also shown. Subsequent contours differ by 0.010. Dashed contours indicate a negative density.

The phonon momentum distribution is given by[6]

$$\rho(\sigma\vec{q})=\sum_{n\vec{k}}F(E(n\vec{k}\sigma))\times\left|\int d^3r\, e^{-i\vec{q}\cdot\vec{r}}\psi(n\vec{k}\sigma,\vec{r})\psi_{\mathrm{pos}}(\vec{r})\right|^2 . \quad (16)$$

σ denotes the spin of the annihilated electrons and ψ_{pos} is the wave function of the positron. $F(E)$ is the Fermi distribution function. The wave function of the positron is evaluated in the independent particle approach, neglecting the correlation between the positron and the electrons which locally alters the electronic structure. Details can be found elsewhere.[7]

As a test case we have evaluated $\rho(\sigma\vec{q})$ for bcc iron using Manning's potential as given by Wood[12,13] which was made ferromagnetic by applying a simple rigid Stoner shift. In Figs. 1(a)–1(c) we compare our results with the results of an *ab initio* KKR calculation done by Rabou.[14] The overall structure is well reproduced and Fermi-surface breaks are identical in position. By construction, the correspondence at points of high symmetry is exact. Exponentially growing errors occur in those regions in reciprocal space, which connect the domains of the separate interpolations. By comparing the values of the matrix elements in the 55 *ab initio* points used for the construction of the model Hamiltonians[5] we find an average absolute error in the matrix elements equal to 3% of their maximum value. Locally in reciprocal space this error can be larger, as is shown in Figs. 1(a)–1(c). Since the interpolated values oscillate around the *ab initio* values, integration in reciprocal space is favorable for reducing the errors. The areas underneath the curves in Figs. 1(a)–1(c) de-

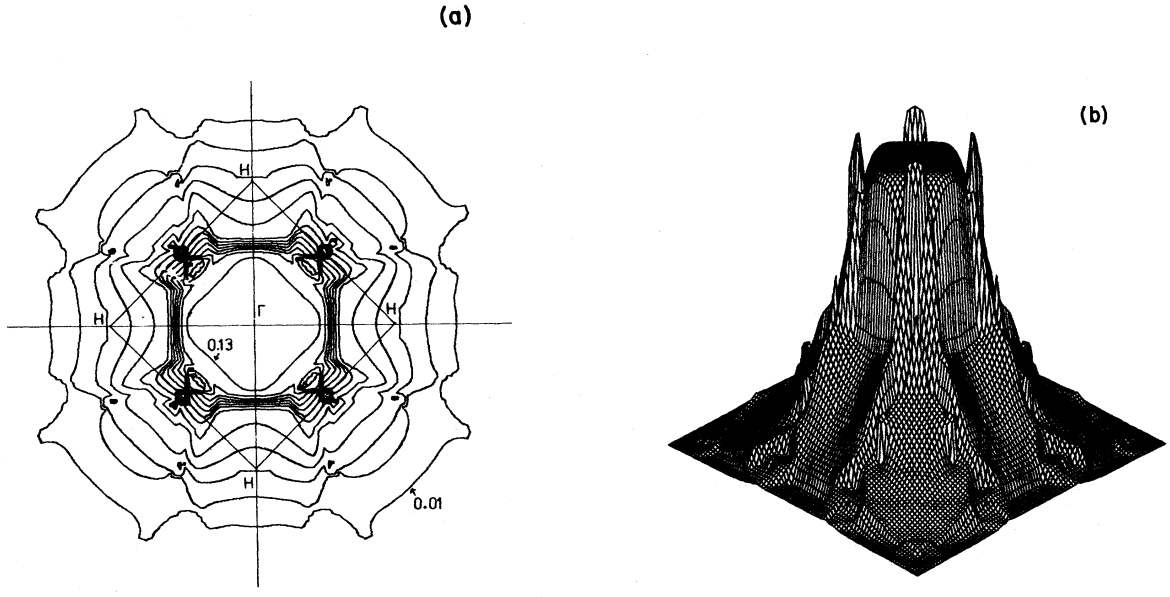

FIG. 7. (a) Contours of the total, normalized, positron-annihilated momentum density, $[N_{\uparrow}^{-1}\rho(\uparrow,\vec{q}(+N_{\downarrow}^{-1}\rho(\downarrow,\vec{q})]/2$, in a (100) plane. First Brillouin zone is also shown. Subsequent contours differ by 0.010. (b) Three-dimensional plot of (a).

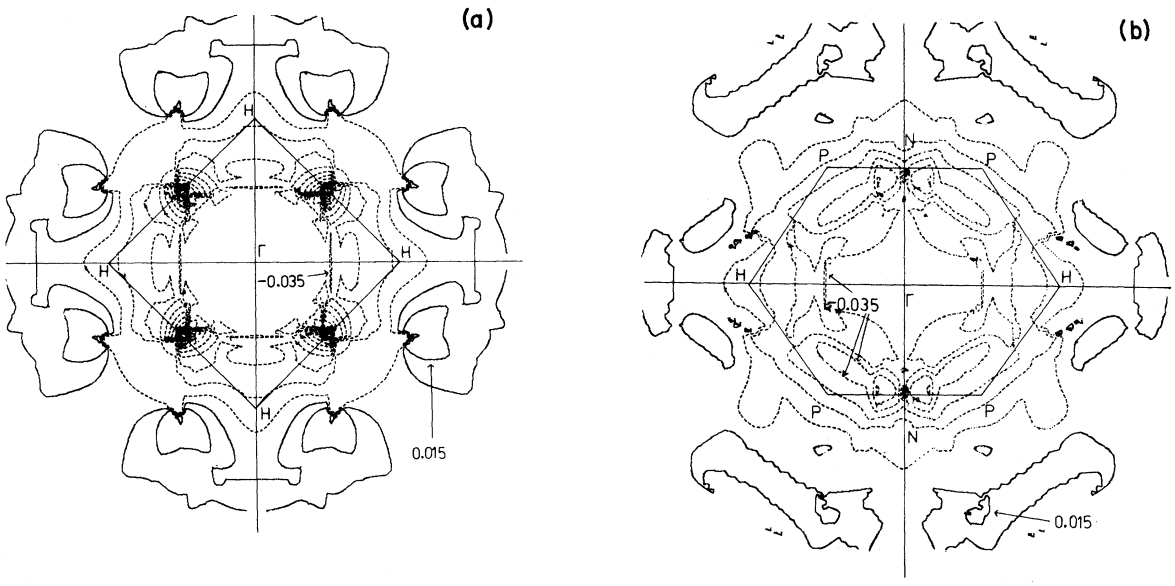

FIG. 8. (a) Contours of the spin difference of the normalized positron annihilation densities, $N_{\uparrow}^{-1}\rho(\uparrow\vec{q})$ $-N_{\downarrow}^{-1}\rho(\downarrow,\vec{q})$, in a (100) plane. First Brillouin zone is also shown. Subsequent contours differ by 0.010. Dashed contours indicate negative values. (b) Similar to (a) in a (110) plane.

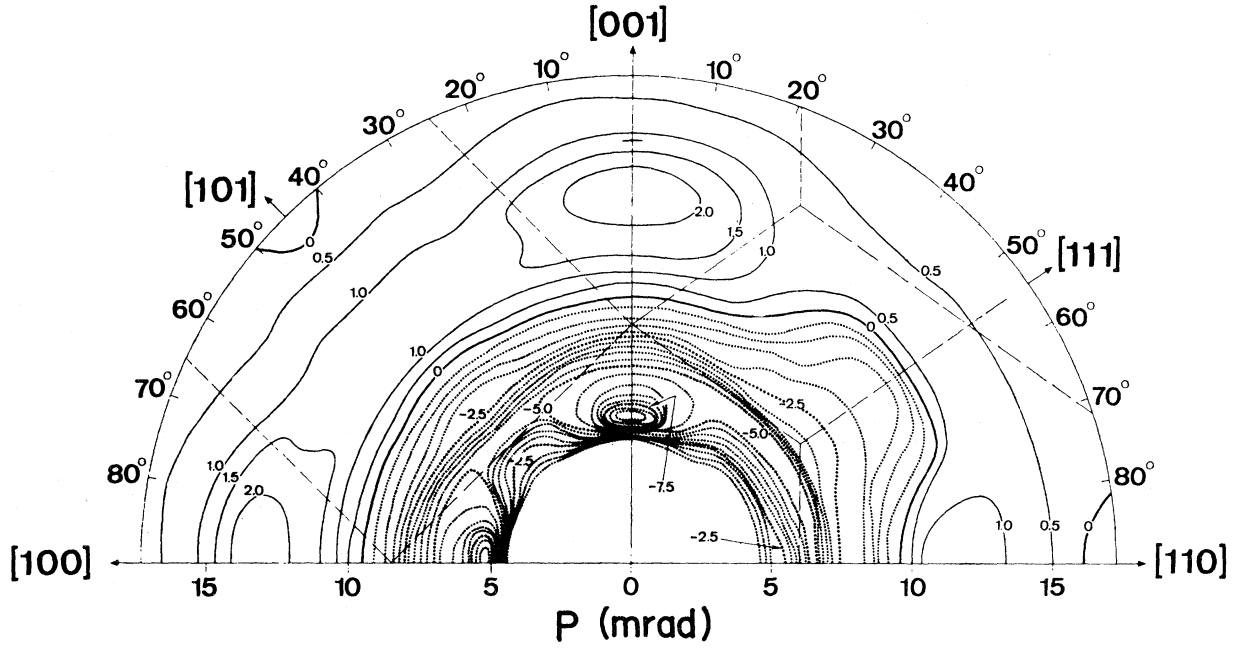

FIG. 9. Contour diagram of the spin difference of the normalized positron annihilation densities as reconstructed from the experiment (Ref. 9). Broken lines represent the Brillouin-zone boundaries.

viate by 3% to 10%, where the relative error is largest when the total area is small.

V. POSITRON ANNIHILATION PROFILES FOR FERROMAGNETIC IRON

In this section we present theoretical results for positron annihilation experiments in ferromagnetic iron. The electronic structure of ferromagnetic iron is derived from a parametrized model potential, which is constructed to yield accurate results for de Haas–van Alphen technique measurements.[7,8] In the standard type of positron annihilation experiments using long-slit detectors one measures the twice-integrated photon momentum distribution

$$N(\sigma\hat{s},s)=N_\sigma^{-1}\int d^3q\,\rho(\sigma\vec{q})\delta(\hat{s}\cdot\vec{q}-s)\,, \qquad (17)$$

which is normalized by

$$N_\sigma=\int d^3q\,\rho(\sigma\vec{q})\,. \qquad (18)$$

The crystal direction $\hat{s}$ coincides with the z axis of the experimental apparatus, along which axis one of the detectors can be moved. The annihilation with the core electrons is neglected in the theoretical curves. Since core electrons are localized, their contribution to the momentum distribution is long range in reciprocal space and the addition of this contribution will effectively lower the central part of the theoretical curves. However, the effect of the core levels on the normalized profiles is only small, especially when one considers the differences between the profiles.

Figure 2 shows the theoretical and experimental results[15] for the twice-integrated spectra for $\hat{s}$ near a [100] direction. The theoretical calculations underestimate the density for small values of q and hence the annihilation with the s-p–like electrons. Due to the correlation between the electrons and the positrons the electronic density in the interstitial region near the positron is increased. Figure 3 shows the difference of the majority-spin and minority-spin profiles for this direction. The agreement between experiment and theory is good and predicts an effective polarization of the positron of about 15%. Figure 4 gives the differences of the profiles for two directions, $N(\sigma\hat{s}_1,s)-N(\sigma\hat{s}_2,s)$, with $\hat{s}_1$ near [211] and $\hat{s}_2$ near [421]. Since these differences are about 1% of the total signal, the inaccuracy of the matrix elements obscures the relation between the experimental and theoretical results. Also, the cancellation of errors stemming from the connecting regions in reciprocal space is less effective when the profiles are taken in different directions.

Once-integrated momentum distributions are displayed in Figs. 5 and 6 for comparison with future experiments. They are obtained from

$$N(\sigma,\vec{s},\vec{t})=N_\sigma^{-1}\int d^3q\,\rho(\sigma\vec{q})\delta(\hat{s}\cdot\vec{q}-\vec{s})\times\delta(\hat{t}\cdot\vec{q}-\vec{t})\,, \qquad (19)$$

and are normalized because of (18). The peaks in the $\langle 11\bar{2}\rangle$ directions are related to the band structure near N, which has large s-p character near the Fermi level. These features are possibly large enough to be detectable in experiments using array counters.

The normalized positron annihilation momentum density $N_\sigma^{-1}\rho(\sigma\vec{q})$ itself is shown in Figs. 7 and 8, while Fig. 9 gives the experimentally determined spin density.[9] The overall agreement is good and the only large difference is found in the negative peaks along the $\langle 110\rangle$ directions. These features cannot be resolved in the construction of Fig. 9 from the experimental data because of their localized character.

VI. CONCLUSIONS

In this paper we have shown that a generalized $\vec{k}\cdot\vec{p}$ interpolation method can be utilized to extract accurate wave functions in a fast, simple, and efficient manner. The accuracy of the model wave functions is 1 order of magnitude less than that of the underlying eigenvalues. In the connecting regions between the separate fits centered on different points of high symmetry the errors in the wave functions are more pronounced than the errors in the energy eigenvalues. The use of our generalized $\vec{k}\cdot\vec{p}$ interpolation scheme enables the calculation of large numbers of matrix elements of complicated materials. Finally, we hope to have stimulated the investigation of ferromagnetic iron by means of two-dimensional positron annihilation experiments.

ACKNOWLEDGMENTS

We would like to thank Dr. L. Rabou and Dr. P. E. Mijnarends for very useful and stimulating discussions and for giving us their theoretical and experimental results. We wish to thank Dr. S. Ber-

ko, Dr. A. A. Manuel, and Dr. A. Th. van Kessel for helpful discussions. This work was part of the research program of the Stichting voor Fundamenteel Onderzoek der Materie (FOM) and received financial support through the Nederlandse Organisatie voor Zuiver Wetenschappelijk Onderzoek (ZWO).

---

*Present address: Department of Physics, Northwestern University, Evanston, IL 60201.

[1]W. A. Harrison, *Pseudopotentials in the Theory of Metals* (Benjamin, New York, 1961).
[2]J. C. Slater and G. F. Koster, Phys. Rev. 94, 1498 (1954).
[3]F. M. Mueller, Phys. Rev. 153, 659 (1967).
[4]See, for example, J. Callaway, *Quantum Theory of Solids* (Academic, New York, 1974), Secs. A and B.
[5]H. J. F. Jansen and F. M. Mueller, Phys. Rev. B 20, 1426 (1979).
[6]P. E. Mijnarends, in *Positrons in Solids,* edited by P. Hautojärvi (Springer, Heidelberg, 1979).
[7]H. J. F. Jansen, Thesis, University of Groningen (1981) (unpublished).
[8]H. J. F. Jansen, G. G. Lonzarich, and F. M. Mueller, in *Physics of Transition Metals, 1980,* edited by P. Rhodes (Institute of Physics, London, 1981).
[9]P. E. Mijnarends, Physica (Utrecht) 63, 248 (1973).
[10]J. P. van Dijke, Phys. Rev. B 4, 3375 (1971).
[11]P. O. Löwdin, J. Chem. Phys. 19, 1396 (1951).
[12]M. F. Manning, Phys. Rev. 63, 190 (1943).
[13]J. H. Wood, Phys. Rev. 126, 517 (1962).
[14]L. Rabou, private communication.
[15]P. E. Mijnarends, private communication.